Research Article
Turkish Journal of Maritime and Marine Sciences

DOI: 10.52998/trjmms.1268375
Volume: 9 Issue: 1 (2023) 43-53

A Mesh Convergence Study on 2-D Air Bubble Barrier Simulation with Mean of Inlet Static Pressure and Horizontal Surface Velocity

Ortalama Giriş Statik Basıncı ve Yatay Yüzey Hızı ile 2-Boyutlu Hava Kabarcığı Bariyeri Simülasyonu Üzerinde Bir Ağ Yakınsama Çalışması

Türk Denizcilik ve Deniz Bilimleri Dergisi

Cilt: 9 Sayı: 1 (2023) 43-53

Canberk HAZAR[1,2*], Ali Cemal TÖZ[1]

[1] *Dokuz Eylul University, Maritime Faculty, Izmir, Turkey*
[2]*Zonguldak Bülent Ecevit University, Maritime Faculty, Zonguldak, Turkey*

ABSTRACT

Timing is vital for oil spill response operations. However, deployment of the traditional response equipment, unfortunately, takes much more time. Therefore, innovative solutions are needed to minimize time losses. One of these innovative solutions is the air bubble barrier. Air bubble barrier creates a barrier to anything floating in the water, especially keeping the floating oil and petroleum in the area where it is spilled. Computational Fluid Dynamics simulation has grown in importance as a resource for air bubble barrier studies in recent years. Despite the extraordinary success of Reynolds Averaged Navier-Stoke applications on air bubble barriers, just a few studies concentrate on mesh sensitivity, one of the most fundamental issues with CFD methods. The main purpose of this study is to perform a mesh convergence study by simulating an air bubble barrier in the Simcenter STAR CCM+ software. In this context, in this simulation, a 2D numerical model is considered. The mesh convergence study has been performed by calculating the aperture inlet mean static pressure and the mean horizontal surface velocity. As a result, it is evident that the mesh base size and number of elements in mesh in case 10 can be employed to maintain the solution time-optimal state in the upcoming numerical simulations on the 2D and 3D air bubble barrier. Case 10 represents the mesh base size of 0.015 and the number of elements in mesh of 99042. Findings from this parametric study will be incorporated as mesh control rules into the subsequent 2D and 3D simulations of the air bubble barrier.

Keywords: Oil Spill, Oil Containment Barriers, Air Bubble Barrier, Mesh Convergence, Computational Fluid Dynamics

Article Info
Received: 20 March 2023
Revised: 02 May 2023
Accepted: 03 May 2023

* (corresponding author)
E-mail: canberk.hazar@deu.edu.tr

To cite this article: Hazar, C., Töz, A.C., (2023). A Mesh Convergence Study on 2-D Air Bubble Barrier Simulation with Mean of Inlet Static Pressure and Horizontal Surface Velocity, *Turkish Journal of Maritime and Marine Science* 9(1): 43-53. doi: 10.52998/trjmms.1268375.

ÖZET

Petrol sızıntısı müdahale operasyonları için zamanlama çok önemlidir. Ancak, geleneksel müdahale ekipmanının konuşlandırılması maalesef çok daha fazla zaman almaktadır. Bu nedenle, zaman kayıplarını en aza indirgemek için yenilikçi çözümlere ihtiyaç vardır. Bu yenilikçi çözümlerden biri de hava kabarcığı bariyeridir. Hava kabarcığı bariyeri, suda yüzen her şeye karşı bir bariyer oluşturur, özellikle yüzen petrolü ve petrolü döküldüğü alanda tutar. Hesaplamalı Akışkanlar Dinamiği simülasyonu, son yıllarda hava kabarcığı bariyeri çalışmaları için bir kaynak olarak önem kazanmıştır. Hava kabarcığı bariyerlerinde Reynolds Ortalamalı Navier-Stokes uygulamalarının olağanüstü başarısına rağmen, HAD yöntemlerinin en temel sorunlarından biri olan ağ hassasiyetine odaklanan çok az çalışma vardır. Bu çalışmanın temel amacı, Simcenter STAR CCM+ yazılımında bir hava kabarcığı bariyerini simüle ederek bir ağ yakınsama çalışması yapmaktır. Bu kapsamda bu simülasyonda 2D sayısal model ele alınmıştır. Ağ yakınsama çalışması, nozul girişi ortalama statik basıncı ve ortalama yatay yüzey hızı hesaplanarak gerçekleştirilmiştir. Sonuç olarak, 2D ve 3D hava kabarcığı bariyeri üzerinde gelecek sayısal simülasyonlarda çözüm süresi-en uygun durumunu korumak için durum 10'daki ağ taban boyutunun ve ağ elemanı sayısının kullanılabileceği açıktır. Durum 10, 0.015'lik ağ taban boyutunu ve 99042'lik ağdaki eleman sayısını temsil eder. Bu parametrik çalışmadan elde edilen bulgular, ağ kontrol kuralları olarak hava kabarcığı bariyerinin sonraki 2B ve 3B simülasyonlarına dahil edilecektir.

Anahtar sözcükler: Petrol Sızıntısı, Petrol Tutma Bariyerleri, Hava Kabarcığı Bariyeri, Ağ Yakınsama, Hesaplamalı Akışkanlar Dinamiği

1. INTRODUCTION

One of the biggest threats to the marine ecosystem is oil spills, and there is only a very small window of time to take action to reduce oil pollution (Gündüz and Sözer, 2022). This has caused continual efforts to improve methods for reducing oil pollution. Conventional oil barriers are typically utilized as a part of the chosen pollution reduction technique to confine floating oil (McClimans *et al*., 2013). The pneumatic barrier is an alternative strategy for reducing oil pollution and a way to manage oil spills. It is also known as an air curtain and a bubble curtain.

Brasher employed the air bubble barrier as a mobile breakwater for the first time in 1907. Numerous experts and scientists have tested the usage of the air bubble barrier for numerous reasons through experimental and numerical investigations (Zhang and Bai, 2012). The air bubble barrier was initially investigated as a kind of breakwater (Taylor, 1955). In order to keep freshwater and saltwater from combining at the meeting of rivers and seas, it was investigated in the 1960s (Simmons, 1967). It has also been researched for use in the winter to keep ports clear of ice and avoid sediment buildup in sensitive areas (Bulson, 1961). The efficiency of the air bubble barrier in oil pollution containment was studied after the 1970s when it first started to be researched as an oil containment barrier (Grace and Sowyrda, 1970). The next studies looked into how well it protected ports from oil spills (Lo, 1997).

The first large-scale experiments with the air bubble barrier in homogeneous water were made by Bulson (1961). He found the relationship between the added airflow (q) and the surface velocity (v) created by the bubble, expressed in equation 1:

$$v = k.\left[\frac{gq}{1+D/H_0}\right]^{1/3} \quad (1)$$

Where q is the volume flow of air added per meter of pipe, g is the acceleration of gravity, k is the proportionality coefficient, D is the depth of the air pipe, and H_0 is the water height equivalent to atmospheric pressure. Bulson's experiments gave a k-value of 1.46 when the surface velocity was measured at a distance from the air pipe equal to the depth of the pipe.

Air bubble barriers are created by the release of

air bubbles underwater; air bubbles rise to the surface forming a bubble plume. This plume drags water with it and creates an upward current. When the upward current of water strikes the surface, it changes direction, and a surface flow is produced. Consequently, oil spillage controlled by convection action can be avoided and oil spill is anticipated to be confined in a controlled area. This starts the improvement of a new type of oil barrier. Bubble barriers are generally set up completely underwater. For this reason, the air bubble barrier is less susceptible to ambient wind and wave situations than traditional oil barriers placed on the water's surface, and it often has no impact on ship navigation when in use (Lu *et al*., 2015).

In recent years, CFD tools and methodology have improved extremely. In this regard, CFD simulation has become a major tool in air bubble barrier studies (Xu *et al*., 2019; Lu *et al*., 2015; Wang *et al*., 2019; Fujita, 2016; Yin *et al*., 2020). Although the air bubble barrier has been researched for many different reasons up to this point, it has mostly been investigated so for wave dissipation performance and prevention of oil pollution spread (Hazar and Toz, 2022). Some of the air bubble barrier studies that have been done in recent years using CFD simulation are given. Lu *et al*. (2015) have performed comprehensive analyzes on the reliability of bubble barriers on prevent oil pollution spread, using laboratory experiments and computational simulations. For computational simulation, they have made use of the commercial software program ANSYS FLUENT. A multiphase Navier-Stokes solver, in which air, water, and oil are handled in three various phases using volume of fluid (VOF) technology, is solved using the finite volume method. Turbulence has been modeled using the standard k-ε model. Fujita (2016) concentrates on the air curtain emplaced close to a vertical wall, aimed at implementation to protect land facilities. 2D and 3D numerical simulations have been conducted using OpenFOAM CFD software. InterFoam, a solvent for 2 incompressible liquids, has been utilized for computational simulation. Xu *et al*. (2019) have run numerical simulations to examine the hydrodynamic performance of the pneumatic breakwater. To simulate the current zone surrounding the pneumatic breakwater, they merged the RANS equations with the Shear Stress Transport (SST) k-ω turbulence model. Zang and Bai (2012), Zang (2013), and Zang (2014) have conducted a numerical simulation of the air bubble breakwater. They have regarded the two-phase fluid consisting of air and water as a fluid of variable density. Continuity equation, RANS equations, and standard k-ε turbulence model equations have been chosen as the main equations and the interface of water and air has been monitored by the VOF method. Zhang *et al*. (2010) have examined the wave dispersion performance of the air barrier with various layouts utilizing computational methods. The RANS equation and standard k-ε turbulence model equations have been accepted as the basic equations in the numerical model, which uses the VOF approach to monitor the two-phase interface. Wang *et al*. (2019) have tried to merge submerged breakwater (SB) and pneumatic breakwater (PB) to enhance the efficiency of wave damping for long-period waves. A mathematical model based on RANS equations, the Renormalization Group (RNG) k-ε turbulence model, and the VOF method has been validated through a series of laboratory tests involving PB, SB, and their joint breakwater (JB). Yin *et al*. (2020) have carried out several laboratory tests with two-dimensional (2-D) computational modeling to research the hydrodynamic properties of a PB under the effect of wave currents. The mathematical model has been organized from the RANS equations, the RNG k-ε turbulence model, and the VOF method. RANS and RNG k-ε turbulence model equations have been utilized in that paper to model wave movements and turbulence. The VOF technique has been used for wave surface monitoring. It can be deduced from the studies that RANS equations, the k-ε turbulence model or k–ω SST model, and the VOF method are used in common when creating a mathematical model for the air bubble barrier. Therefore, in this article, the same equations and methods have been used while creating the mathematical model.

Despite the extraordinary achievement of RANS applications on air bubble barriers, few articles focus on mesh sensitivity, one of the most

important issues with CFD methods. Mesh convergence is a crucial factor to take into account in CFD simulations (Jiang *et al*., 2022). The number of elements needed in a model to ensure that changing the mesh size has no impact on the analysis findings is determined by mesh convergence. After convergence, further mesh refining has no impact on the outcomes. The model and its outputs are now independent of the mesh (Gardiner, 2017). Many studies address the mesh convergence from various sectors such as mechanical engineering (Zadeh *et al*., 2014; Sanjaya *et al*., 2021; Patil and Jeyakarthikeyan, 2018; Devals *et al*., 2016; Naik *et al*., 2019), advanced materials and structures (Tso *et al*., 2012; Molitoris *et al*., 2014; Bjorkman and Molitoris, 2012; Vales and Kala, 2018), aeronautics (Lozano, 2019; Loseille *et al*., 2007; Puggelli *et al*., 2023), civil engineering (Wang, 2014; Ghavidel *et al*., 2020), wind farm (Gargollo-Peiro *et al*., 2018; Gargollo-Peiro *et al*., 2022) numerical methods in engineering (Bishop and Strack, 2011; Taraschi and Correa, 2022). On the other hand, mesh convergence continues to be a significant challenge when the RANS technique is utilized to solve complicated turbulence that is beyond the capabilities of the computational model. In addition, although CFD applications in air bubble barrier studies have developed, no studies are focusing on mesh sensitivity. Therefore, this study focuses on mesh sensitivity in CFD applications of air bubble barriers.

This study aims to make a mesh convergence study of this model by constructing a 2D numerical model to numerically simulate the air bubble barrier and calculate the aperture inlet average static pressure and average horizontal surface velocity. RANS equations solver using the standard k-ω SST turbulence model will be performed for all analyses. The k- ω SST model is chosen because it provides a better flow separation estimation than other RANS models and has a higher accuracy/expense ratio than other turbulence models used in the industry (Menter,1992). The study is organized as follows: first, information about the air bubble barrier and the background is given. In the second chapter, the numerical model will be explained and in the third part, the results will be given. In the fourth part, the study will be concluded.

2. MATERIAL AND METHOD

This chapter presents the 2-D mathematical model, governing equations, boundary conditions, and solution algorithms in Simcenter STAR CCM+ software. A numerical model is proposed to simulate the air bubble barrier numerically and to perform the mesh convergence study. The schema of the 2-D numerical model (3.6 x 1.2 [m]: L x D) that is analyzed in this study is given in Figure 1. The aperture inlet is defined as the boundary where the air intake is in the numerical model.

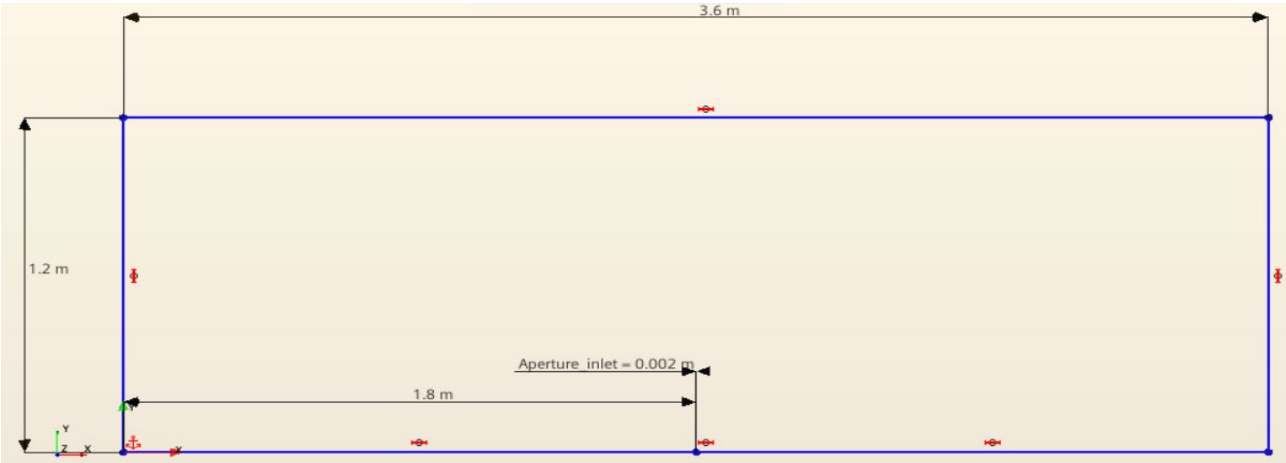

Figure 1. The schema of the 2-D numerical model and aperture inlet

A multiphase RANS equations solver in which air and water are handled as two distinct phases using VOF technology is solved using the finite volume method. The k–ω SST model is used to model turbulence. The VOF model is modeled by the Eulerian approach. The aperture on the air bubble barrier is used as the velocity input. A pressure outlet is used above the calculation area, i.e., open to the air. Wall boundary condition was used on the bottom and sides of the model (Xu *et al*., 2019). The boundary conditions of the 2-D numerical model are given in Table 1. In the analysis, the density and dynamic viscosity of water is taken as 997.561 kg/m^3 and 8.8x10^{-4} Pa-s, respectively. The density and dynamic viscosity of air is taken as 1 kg/m^3 and 1.85x10^{-5} Pa-s, in turn.

Table 1. Boundary conditions of the 2-D numerical model

Part surfaces	Type
Aperture Inlet	Mass flow inlet
Outlet (open to the air)	Pressure outlet
Bottom and sides of the model	No slip wall

For the solution, automated mesh (2D) and unstructured mesh are selected. Then, polygonal (polygonal) mesh and prism layer mesh is selected. Polygonal mesh is used to divide the digital model into regions with different mesh resolutions. For the mesh convergence study, the base size is initially taken as 0.08 m. Afterward, the base size was reduced until the mean of aperture inlet static pressure and horizontal surface velocity values converged. The analysis was terminated at the point where the mean of aperture inlet static pressure and horizontal surface values converged. In Table 2, the mesh base size and number of elements in the mesh are given. While creating the mesh, the number of prism layers is 2 and the total thickness of the prism layer is taken as 33.33% of the base size. The number of prism layers and the total thickness of the prism layer have been adjusted according to the formation of a smooth mesh image at the aperture inlet.

Table 2. Mesh base size and number of elements in the mesh

Case No	Mesh base size (m)	Number of elements in the mesh
1	0.08	7208
2	0.07	9625
3	0.06	11293
4	0.05	12776
5	0.04	21751
6	0.03	33393
7	0.023	41199
8	0.0205	54806
9	0.02	70117
10	0.015	99042
11	0.013	109966
12	0.0112	122821

In the initial conditions, there is 1-meter-deep water in the tank and the tank is open to the atmosphere. The air bubble barrier is positioned at the bottom of the model. The initial conditions are shown in Table 3. The aperture diameter of the air bubble barrier is 0.002 m, and the mass flow rate of air is taken as 0.02 kg/s. Figure 4 clearly shows that the mean static pressure values start to converge in about 0.1 seconds in each mesh number, so the numerical simulation is run for 5 seconds after it started to converge.

Table 3. Initial conditions of the 2-D numerical model

Water height	1 m
Velocity	[0.0,0.0] m/s
Pressure	0.0 Pa
Turbulence intensity	0.01
Turbulence specification method	Intensity + Viscosity Ratio
Turbulent Velocity Scale	1.0 m/s
Turbulent viscosity ratio	10
Aperture diameter	0.002 m
The mass flow rate of air	0.02 kg/s

For the mesh convergence study, the mean static pressure at the aperture inlet of the air bubble barrier and the mean horizontal surface velocity at the water surface has been calculated. To calculate the mean static pressure at the aperture inlet of the air bubble barrier for 5 seconds, 25 line probes were positioned vertically up to the water surface in the middle of the model, and the

mean horizontal surface velocity for 5 seconds, 150 line probes have been placed 0.05 meters below the water surface along the water surface and the velocity at each line probe has been averaged. The volume fraction of water and position of the line probes in the numerical model at initial conditions are given in Figures 2 (a) and 2 (b).

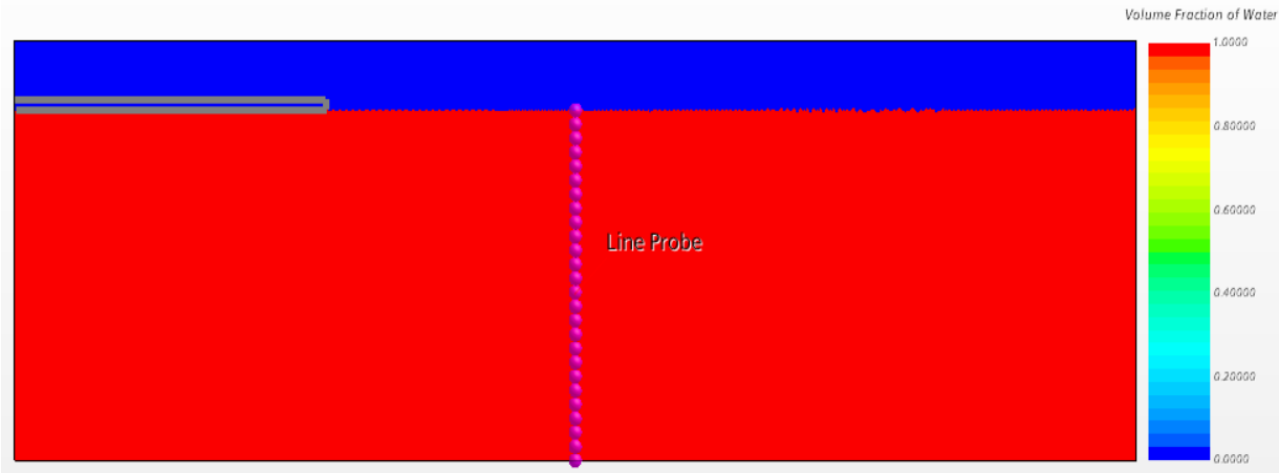

Figure 2 (a). The volume fraction of water and position of the line probes in the numerical model at initial conditions for mean static pressure (t=0 s)

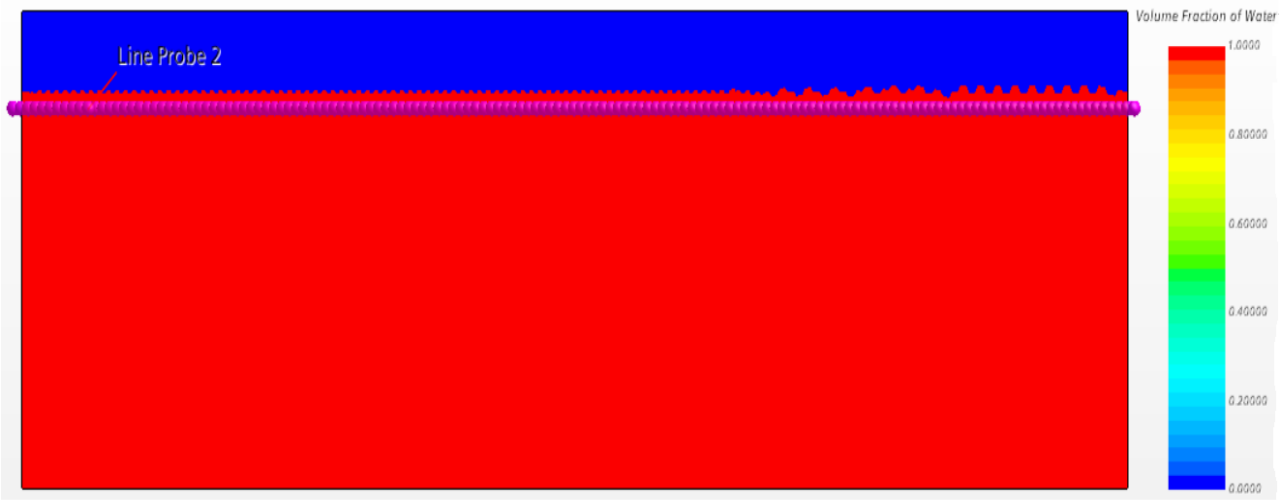

Figure 2 (b). The volume fraction of water and position of the line probes in the numerical model at initial conditions for mean horizontal surface velocity (t=0 s)

3. RESULTS AND DISCUSSION

In this section, validation of the numerical analysis and the outputs of the mesh convergence study for the different number of elements in the mesh is given. The aperture inlet mean static pressure and mean horizontal surface velocity of the air bubble barrier are analyzed for the different numbers of elements in the mesh. The data obtained from the Star CCM+ have been first exported to Excel. Afterward, the data in Excel has been imported the MATLAB, and graphs have been created. The resolution of the graphics has been optimally adjusted using the GIMP image processing software.

3.1. Validation of Numerical Analysis

The validation of the numerical analysis is made employing Equation 1 given in the introduction section. By taking the mass flow rates of 0.01, 0.02, 0.03, and 0.04 kg/s, the highest mean

surface velocities are found for each analysis. According to Equation 1, the ratio of the surface velocities encountered to each other should be 1. Numerical model validation has been done using Mean Absolute Percentage Error (MAPE). The MAPE formula is expressed in Equation 2.

$$M = \frac{1}{n}\sum_{t=1}^{n}\left|\frac{A_t - F_t}{A_t}\right| \quad (2)$$

where A_t is the actual value and F_t is the forecast value. Their difference is divided by the actual value A_t. The absolute value of this ratio is summed for every forecasted point in time and divided by the number of fitted points n. The F_t value is taken as 1 according to the 1/3-power law (Eidnes *et al.*, 2013).

Table 4 shows the highest mean surface velocities calculated in the case of different pollutants, the absolute error values by the actual value, and the MAPE value. The MAPE value of 5.77% indicates that the numerical model works with high accuracy.

Table 4. Validation of numerical analysis

Pollutants	Highest mean surface velocity (m/s)			
Gasoline	0,3852	0,5435	0,6666	0,6952
Diesel	0,4404	0,4790	0,6564	0,7251
Fuel oil	0,4174	0,5479	0,6393	0,7073
Average	0,4143	0,5235	0,6541	0,7092
At	1,0811	1,0771	1,0273	
Ft	1	1	1	
The ratio of mass flow rate	0.02/0.01	0.03/0.02	0.04/0.03	Total
Abs. Of error by actual value	0,0750	0,0716	0,0266	0,1731
			MAPE	**5,77%**

3.2. Results

The aperture inlet mean static pressure values of the air bubble barrier for the different number of elements in the mesh are presented in Figure 4. Figure 3 clearly shows that the mean static pressure values start to converge around 0.1 seconds in each mesh number, and after 0.1 seconds, the mean static pressure values remain at 9800 Pa. Mean static pressure values between 0 and 0.05 are shown in an enlarged or zoomed-in manner on the left side in Figure 3.

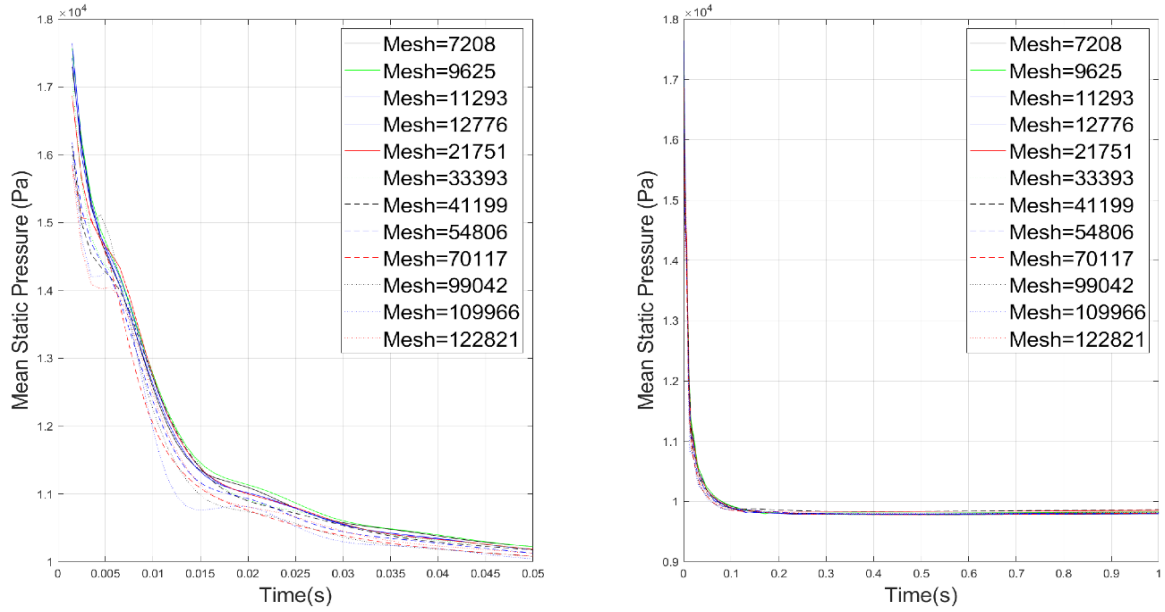

Figure 3. The mean static pressure values of the air bubble barrier for different numbers of elements in the mesh

The mean horizontal surface velocity values along the water surface of the air bubble barrier for the different number of elements in the mesh are presented in Figure 4. Figure 4 demonstrates that the mean horizontal surface velocity values fluctuate until they converge at a certain number of elements in the mesh.

Figure 5 shows the mean horizontal surface velocity values from cases 1 to 9 and the mean horizontal surface velocity values from cases 10 to 12, separately. As can be seen from Figure 5, the mean horizontal surface velocity values converge from case 10 to case 12. The highest mean horizontal surface velocity values are 0.06 m/s. In case 12, the numerical analysis is terminated. In addition, when we look at the average of the mean horizontal surface velocity values for each case, it is seen that the average of mean horizontal surface velocity values converges since case 8. In Figure 6, it is evident that the mean of the mean horizontal surface velocity values converged around 0.003 m/s after case 8.

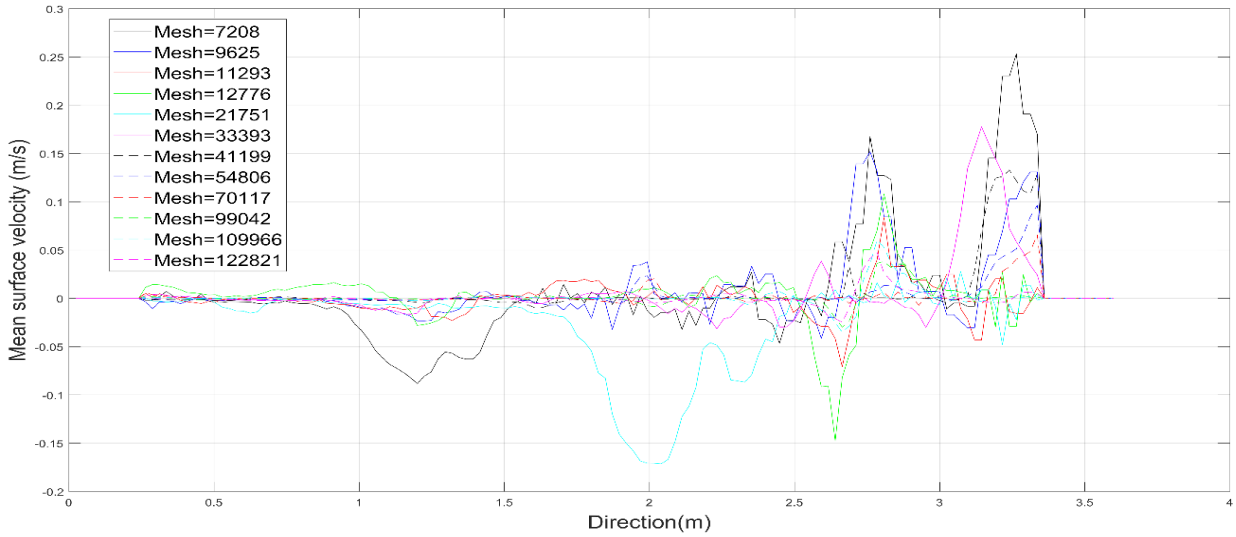

Figure 4. The mean horizontal surface velocity values along the water surface of the air bubble barrier for different numbers of elements in the mesh

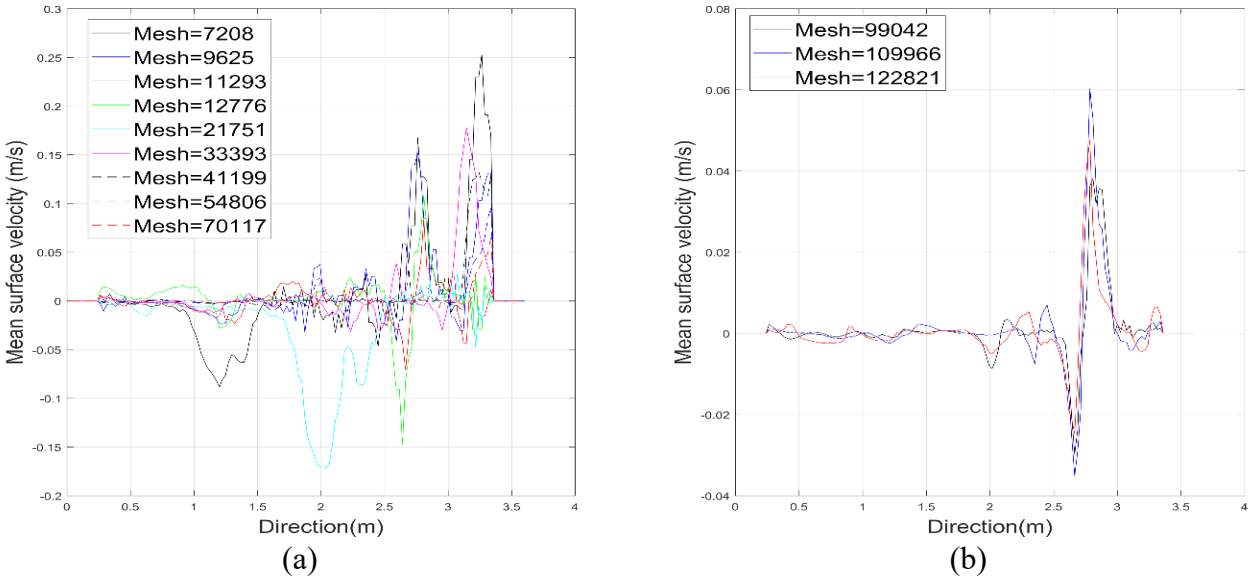

Figure 5. The mean horizontal surface velocity values along the water surface of the air bubble barrier from (a) cases 1 to 9 and (b) cases 10 to 12.

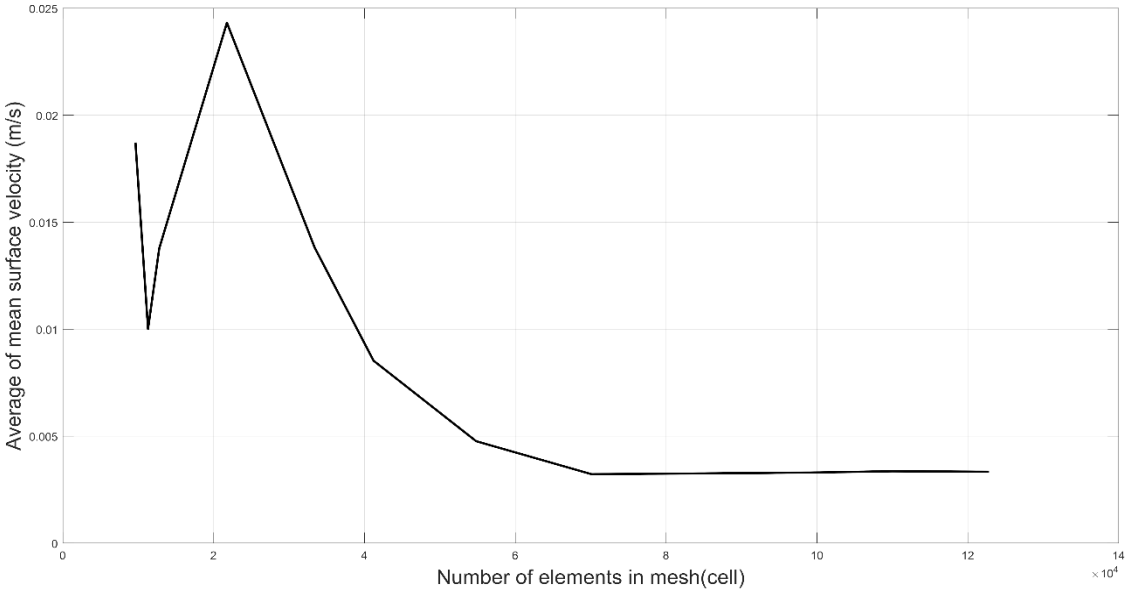

Figure 6. The average of mean horizontal surface velocity values along the water surface of the air bubble barrier for the different number of elements in the mesh.

4. CONCLUSION

This paper presents a mesh convergence study to form the basis for subsequent 2D and 3D air bubble barrier numerical simulations. In this study, a 2D numerical model is proposed to numerically simulate the air bubble barrier and a mesh convergence study of this model is performed by calculating the aperture inlet mean static pressure and mean horizontal surface velocity.

The convergence of the aperture inlet mean static pressure at 9800 Pa shows that the numerical simulation is working correctly. Because this static pressure value also meets the static pressure value at the bottom of the water, which is calculated $P = \rho g h$ formula. At the same time, it is seen that the numerical simulation starts to converge after 0.1 seconds in all cases. After the convergence started, the numerical simulation has been run for another 5 seconds. Considering the mean horizontal surface velocity values, a convergence is observed after case 10. When we look at the mean horizontal surface velocity values, there is fluctuation in the values up to case 9, but a convergence could be reached between case 10 and case 12.

Consequently, it is seen that the mesh base size and the number of elements in mesh in case 10 can be used to keep the solution time-optimal in the next numerical simulations to be made on 2-D and 3-D air-bubble barriers. The outputs are anticipated to serve as a useful reference for computational simulation of the air bubble barrier in 2D and 3D models.

AUTHORSHIP CONTRIBUTION STATEMENT

Canberk HAZAR: Conceptualization, Methodology, Validation, Formal Analysis, Resources, Writing - Original Draft, Writing-Review and Editing, Data Curation, Software, Visualization, Supervision, Project administration.

Ali Cemal TÖZ: Conceptualization, Methodology, Validation, Formal Analysis, Resources, Writing - Original Draft, Writing-Review and Editing, Supervision, Project administration.

CONFLICT OF INTERESTS

The author(s) declare that for this article they have no actual, potential, or perceived conflict of interest.

ETHICS COMMITTEE PERMISSION

No ethics committee permission is required for this study.

FUNDING

This work was supported/funded by the DEU Department of Scientific Research Projects with the FDK-2021-2594 project code.

ORCID IDs

Canberk HAZAR:
https://orcid.org/0000-0001-6138-4181
Ali Cemal TÖZ:
https://orcid.org/0000-0001-5348-078X

5. REFERENCES

Bishop, J.E., Strack, O.E., (2011). A statistical method for verifying mesh convergence in Monte Carlo simulations with application to fragmentation. *International Journal for Numerical Methods in Engineering* 88(3): 279-306. doi:10.1002/nme.3176.

Bjorkman, G.S., Molitoris, D.P., 2012. Mesh convergence studies for thin shell elements developed by the ASME Task group on computational modeling. ASME 2011 Pressure Vessels and Piping Conference 57705, pp. 119-123. doi: 10.1115/PVP2011-57705.

Bulson, P.S., (1961). Current produced by an air curtain in deep water. *The Dock and Harbour Authority* 42: 15-22.

Devals, C., Vu, T.V., Zhang, Y., Dompierre, J., Guibault, F., 2016. Mesh convergence study for hydraulic turbine draft-tube. 28th IAHR symposium on Hydraulic Machinery and Systems, 49: 082021. doi: 10.1088/1755-1315/49/8/082021.

Eidnes, G., Leirvik, F., McClimans, T.A., Gjosund, S. H., Grimaldo, E., 2013. Containing oil spills by use of air bubbles. Proceedings of the 2013 International offshore and polar engineering anchorage, Alaska, USA.

Fujita, I., 2016. Bubble curtain for blocking spilled oil on water surface, 2016 Techno-Ocean, pp. 354-359. doi: 10.1109/TechnoOcean.2016.7890678.

Gardiner, J., Finite Element Analysis Convergence and Mesh Independence, (2022). Accessed Date: 10.03.2022, https://www.xceed-eng.com/finite-element-analysis-convergence-and-mesh-independence/ is retrieved.

Gargallo-Peiro, A., Avila, M., Owen, H., Prieto-Godino, L., Folch, A., (2018). Mesh generation, sizing and convergence for onshore and offshore wind farm Atmospheric Boundary Layer flow simulation with actuator discs. *Journal of Computational Physics* 375: 209-227. doi: 10.1016/j.jcp.2018.08.031.

Gargallo-Peiro, A., Revilla, G., Avila, M., Houzeaux, G., (2022). A level set-based actuator disc model for turbine realignment in wind farm simulation: Meshing, convergence and applications. *Energies* 15(23): 1-24. doi: 10.3390/en15238877.

Ghavidel, A., Rashki, M., Ghohani Arab, H., Azhdary Moghaddam, M., (2020). Reliability mesh convergence analysis by introducing expanded control variates. *Frontiers of Structural and Civil Engineering* 14(4): 1012-1023. doi: 10.1007/s11709-020-0631-6.

Grace, J., Sowyrda, A., (1970). The development and evaluation of a pneumatic barrier for restraining surface oils in a river. *Journal of the Water Pollution Control Federation* 42: 2074-2093.

Gündüz, M., Sözer, A., (2022). Modelling the impact of the oil spill pollution in Ildır Bay, Turkey. *Turkish Journal of Maritime and Marine Sciences* 8(1): 60-68. doi: 10.52998/trjmms.1070706.

Hazar, C., Toz, A.C., 2022. Use of air bubble barrier for oil containment: A literature review. Global Conference on Engineering Research (GLOBCER'22) Proceedings Book, pp. 126-133, Turkey.

Jiang, Y., Murray, A., Di Mare, L., Ireland, P., (2022). Mesh sensitivity of RANS simulations on film cooling flow. *International Journal of Heat and Mass Transfer* 182(121825). doi: 10.1016/j.ijheatmasstransfer.2021.121825.

Lo, J.M., (1997). The effect of air bubble barriers in containing oil-slick movement. *Ocean Engineering* 24(7): 645-663.

Loseille, A., Dervieux, A., Frey, P., Alauzet, F., 2007. Achievement of global second order mesh convergence for discontinuous flows with adapted unstructured meshes. 18th AIAA Computational Fluid Dynamics Conference, 4186. doi: 10.2514/6.2007-4186.

Lozano, C., (2019). Watch your adjoints! Lack of mesh convergence in inviscid adjoint solutions. *American Institute of Aeronautics and Astronautics Journal* 57(9): 3991-4006. doi: 10.2514/1.J057259.

Lu, J., Xu, Z., Xu, S., Xie, S., Wu, H., Yang, Z., Liu, X., (2015). Experimental and numerical investigations on reliability of air barrier on oil containment in flowing water. *Marine Pollution Bulletin* 95(1): 200-206. doi: 10.1016/j.marpolbul.2015.04.020.

McClimans, T., Leifer, I., Gjosund, S.H., Grimaldo, E., Daling, P., Leirvik, F., (2013). Pneumatic oil barriers: The promise of area bubble plumes. *Engineering for The Maritime Environment* 227(1): 22-38. doi: 10.1177/14750902124502.

Menter, F.R., 1992. Improved Two-Equation k-omega Turbulence Models for Aerodynamic Flows. NASA Technical Memorandum 103975.

Molitoris, D.P., Bjorkman, G.S., Tso, C.F., Yaksh, M., 2014. Mesh convergence studies for thick shell elements developed by the ASME special working group on computational modeling. ASME 2013 Pressure Vessels and Piping Conference, 97992. doi: 10.1115/PVP2013-97992.

Naik, N., Shenoy, P., Nayak, N., Awasthi, S., Samant, R., (2019). Mesh convergence test for finite element method on high pressure gas turbine disk rim using energy norm: An Alternate approach. *International Journal of Mechanical Engineering and Technology* 10(1): 765-775. doi: 10.34218/IJMET.10.1.2019.078.

Patil, H., Jeyakarthikeyan, P.V., 2018. Mesh convergence study and estimation of discretization error of hub in clutch disc with integration of Ansys. 2nd International conference on Advances in Mechanical Engineering, 402, 012065. doi:10.1088/1757-899X/402/1/012065.

Puggelli, S., Leparoux, J., Brunet, C., Mercier, R., Liberatori, L., Zurbach, S., Cabot, G., Grisch, F., (2023). Application of an automatic mesh convergence procedure for the large eddy simulation of a multipoint injection system. *J. Eng. Gas Turbines Power* 145(6): 061019. doi: 10.1115/1.4056635.

Sanjaya, Y., Prabowo, A.R., Imaduddin, F., Nordin N.A.B., (2021). Design and analysis of mesh size subjected to wheel rim convergence using finite element method. *Procedia Structural Integrity* 33: 51-58. doi: 10.1016/j.prostr.2021.10.008.

Simmons, H.B., 1967. Potential benefits of pneumatic barriers in estuaries. Proceedings, American Society of Civil Engineers, 93, pp. 1-16.

Taraschi, G., Correa, M.R., (2022). On the convergence of the primal hybrid finite element method on quadrilateral meshes. *Applied Numerical Mathematics* 181: 552-560. doi: 10.1016/j.apnum.2022.07.005.

Taylor, G.I., 1955. The action of a surface current used as a breakwater. Proceedings, Royal Society of London, Series A 231, pp. 466-478.

Tso, C.F., Molitoris, D.P., Snow, S., (2012). Propped cantilever mesh convergence study using hexahedral elements. *Packaging, Transport, Storage & Security of Radioactive Material* 23(10-2): 30-35. doi: 10.1179/1746510912Y.0000000011.

Vales, J., Kala, Z., (2018). Mesh convergence study of solid FE model for buckling analysis. AIP Conference Proceedings 1978(1): 150005. doi: 10.1063/1.5043796.

Wang, I.T., (2014). Numerical and experimental verification of finite element mesh convergence under explosion loading. *Journal of Vibroengineering* 16(4): 1786-1798.

Wang, Y., Yin, Z., Liu, Y., Yu, N., Zou, W., (2019). Numerical investigation on combined wave damping effect of pneumatic breakwater and submerged breakwater. *International Journal of Naval Architecture and Ocean Engineering* 11(1): 314-328. doi: 10.1016/j.ijnaoe.2018.06.006.

Xu, T.J., Wang, X.R., Guo, W.J., Dong, G.H., Bi, C.W., (2019). Numerical simulation of the hydrodynamic behavior of a pneumatic breakwater. *Ocean Engineering* 180(9): 108-118. doi: 10.1016/j.oceaneng.2019.04.010.

Yin, Z., Wang, Y., Jia, Q., (2020). Hydrodynamic characteristics of a pneumatic breakwater with combined wave-current actions: A numerical investigation. *Journal of Coastal Research* 36(1): 196-203. doi: 10.2112/JCOASTRES-D-18-00140.1.

Zadeh, S.N., Komeili, M., Paraschivoiu, M., (2014). Mesh convergence study for 2-D straight-blade vertical axis wind turbine simulations and estimation for 3-D simulations. *Transactions of the Canadian Society for Mechanical Engineering* 38(4): 487-504. doi: 10.1139/tcsme-2014-0032.

Zang, C., (2013). Numerical simulation study on the submerged pipe depth of air bubbles breakwater. *Applied Mechanics and Materials* 353-356: 2732-2735. doi:10.4028/www.scientific.net/AMM.353-356.2732.

Zang, C., (2014). Numerical simulation on the wave dissipating performance of air bubbles breakwater with double air discharged pipes. *Applied Mechanics and Materials* 501-504: 2112-2115. doi: 10.4028/www.scientific.net/AMM.501-504.2112.

Zang, C., Bai, L., (2012). Numerical simulation study on the air amount scale of air bubbles breakwater. *Applied Mechanics and Materials* 170-173: 2298-2302. doi:10.4028/www.scientific.net/AMM.170-173.2298.

Zhang, C., Wang, Y., Wang, G., Yu, L., (2010). Wave dissipating performance of air bubble breakwaters with different layouts. *Journal of Hydrodynamics* 22(5): 671-680. doi: 10.1016/S1001-6058(09)60102-5.